Tunable Photoluminescence Wavelength of Chalcopyrite $CuInS_2$-Based Semiconductor Nanocrystals Synthesized in a Colloidal System

Hiroyuki Nakamura,[†] Wataru Kato,[†,§] Masato Uehara,[†] Katsuhiro Nose,[‡] Takahisa Omata,[‡] Shinya Otsuka-Yao-Matsuo,[‡] Masaya Miyazaki,[†,§] and Hideaki Maeda*[,†,§]

Nanotechnology Research Institute, National Institute of Advanced Industrial Science and Technology (AIST), 807-1 Shuku-machi, Tosu, Saga 841-0052, Japan, Department of Materials Science and Processing, Graduate School of Engineering, Osaka University, 2-1 Yamada-oka, Suita 565-0871, Japan, and Department of Molecular and Material Sciences, Interdiscplinary Graduate School of Engineering Sciences, Kyushu University, 6-1 Kasugakoen, 816-8580, Japan

Received August 11, 2005. Revised Manuscript Received February 16, 2006

Chalcopyrite-type $CuInS_2$-based alloyed fluorescent nanocrystals (NCs), which contain no regulated heavy metal ions, were synthesized by heating an organometallic solution to demonstrate optical property tunability. Introduction of Zn into the $CuInS_2$ system enhanced their photoluminescence (PL) intensity. The resultant particles were 3−6 nm; they varied with experimental conditions and were discrete and colloidally stable. The band-gap energy and PL wavelength of Zn-Cu-In-S (ZCIS) NCs varied with Zn content and particle size. Their PL was controllable within 570−800 nm by altering the band-gap energy. Furthermore, indium substitution with gallium was shown to control band-gap energy toward ∼3.1 eV, 500 nm of PL wavelength. In addition, ZnS coating of this nanocrystal can approximately double the PL strength. Finally, surface treatment with mercaptoundecanoic acid dispersed hydrophilic ZCIS NCs into water.

Introduction

Various binary- and singular-type semiconductor nanocrystals (NCs) with high colloidal stability and well-defined particle size distribution have been synthesized during the past decade using solution methods.[1] They are anticipated for use as biomolecular tags, displays, and LEDs[2] and as building blocks of nanomaterials.[3] Among these semiconductors, II−VI-type semiconductors, which favor ionic bonding, are often selected as materials because they offer high quantum yield and the tunable fluorescence wavelength of NCs can be prepared easily. Typically, II−VI-type semiconductor NCs corresponding to visible or near-infrared fluorescence contain Cd, Hg, and Pb. Such heavy metals are becoming difficult to use for public applications; this situation is typified by the "Restriction of the Use of Certain Hazardous Substances (RoHS)" in Europe, which has banned the use of these heavy metals in electrical components.

Apart from these binary semiconductors, multinary semiconductors such as I−III−VI_2-type chalcopyrite materials offer alternatives for appropriate band-gap energies (e.g., 3.4 eV for $CuAlS_2$ and 1.5 eV for $CuInS_2$). Regarding optical aspects, most I−III−VI_2 semiconductors are direct transition semiconductors, and favor ionic bonding, similarly to II−VI-type materials. For bulk materials, control of their properties has been investigated intensively, especially as photovoltaic components of solar cells and recently as photocatalysts.[4] Furthermore, some chalcopyrite materials are sought as tailorable ferromagnetic materials, which are applicable for "spintronics".[5] Many are synthesized using

* To whom correspondence should be addressed. Phone: +81-942-81-3676. Fax: +81-942-81-3657. E-mail: maeda-h@aist.go.jp.
[†] National Institute of Advanced Industrial Science and Technology.
[‡] Osaka University.
[§] Kyushu University.

(1) (a) Henglein, A. *Chem. Rev.* **1989**, *89*, 1861−1873. (b) Murray, C. B.; Norris, D. J.; Bawendi, M. G. *J. Am. Chem. Soc.* **1993**, *115*, 8706−8715. (c) Alivisatos, A. P. *Science* **1996**, *271*, 933−937. (d) Hines, M. A.; Guyot-Sionnest, P. *J. Phys. Chem. B* **1998**, *102*, 3655. (e) Trinidade, T.; O'Brien, P.; Pickett, N. L. *Chem. Mater.* **2001**, *13*, 3843−3858. (f) Qu, L. H.; Peng, Z. A.; Peng, X. G. *Nano Lett.* **2001**, *1*, 331−337. (g) Nakamura, H.; Yamaguchi, Y.; Miyazaki, M.; Maeda, H. *Chem. Commun.* **2002**, 2844−2845. (h) English, D. S.; Pell, L. E.; Yu, Z.; Barbara, P. F.; Korgel, B. A. *Nano Lett.* **2002**, *2*, 681−675. (i) Gerion, D.; Zaitseva, N.; Saw, C.; Casula, M. F.; Fakra, S.; Van Buuren, T.; Galli, G. *Nano Lett.* **2004**, *4*, 597−602. (j) Green, M. *Curr. Opin. Solid State Mater. Sci.* **2002**, *6*, 355−363. (k) Battaglia, D.; Peng, X. *Nano Lett.* **2002**, *2*, 1027−1030. (l) Talapin, D. V.; Rogach, A. L.; Mekis I.; Haubold, S.; Kornowski, A.; Haase, M.; Weller, H. *Colloids Surf. A* **2002**, *202*, 145−154. (m) Micic, O. I.; Ahrenkiel, S. P.; Bertram, D.; Nozik, A. J. *Appl. Phys. Lett.* **1999**, *75*, 478−480.

(2) (a) Klein, D. L.; Roth, R.; Lim, A. K. L.; Alivisatos, A. P.; McEuen, P. L. *Nature* **1997**, *389*, 699. (b) Bruchez, M.; Moronne, M.; Gin, P.; Weiss, S.; Alivisatos, A. P. *Science* **1998**, *281*, 2013. (c) Kirstein, S.; Mohwald, H.; Rogach, A. L.; Kornowski, A.; Eychmuller, A.; Weller, H. *J. Phys. Chem. B* **1998**, *102*, 8360−8363. (d) Chan, W. C. W.; Maxwell, D. J.; Gao, X.; Bailey, R. E.; Han, M.; Nie, S. *Anal. Biotechnol.* **2002**, *13*, 40−46. (e) Kompe, K.; Borchert, H.; Storz, J.; Lobo, A.; Adam, S.; Moller, T.; Haase, M. *Angew. Chem.* **2003**, *42*, 5513−5516. (f) Gao, X.; Cui, Y.; Levenson, R. M.; Chung, L. W. K.; Nie, S. *Nat. Biotechnol.* **2004**, *22*, 969−976. (g) Clemens, B.; Chen, X.; Narayanan, R.; El-Sayed, M. *Chem. Rev.* **2005**, *105*, 1025. (h) Michalet, X.; Pinaud, F. F.; Bentolila, L. A.; Tsay, J. M.; Doose, S.; Li, J. J.; Sundaresan, G.; Wu, A. M.; Gambhir S. S.; Weiss, S. *Science* **2005**, *307*, 538−544.

(3) (a) Boal, A. K.; Ilhan, F.; DeRouchey, J. E.; Thurn-Albrecht, T.; Russell, T. P.; Rotello, V. M. *Nature* **2000**, *404*, 746. (b) Calvert, P. *Chem. Mater.* **2001**, *13*, 3299. (c) Fendler, J. H. *Chem. Mater.* **2001**, *13*, 3196. (d) Zhang, Z. L.; Glotzer, S. C. *Nano Lett.* **2004**, *4*, 1407. (e) Heule, M.; Vuillemin, S.; Gauckler, L. J. *Adv. Mater.* **2003**, *15*, 1237.

10.1021/cm0518022 CCC: $33.50
Published on Web 06/17/2006

gas-phase deposition methods (e.g., sputtering, MBE, MOCVD) and solution methods (e.g., spray pyrolysis, solvothermal method).[6]

Results have been reported widely for bulk and rather large particles, but few studies have examined nonaggregated chalcopyrite nanocrystals (NCs) of a few nanometers, which would be ideal as building blocks of nanomaterials and biological tags.

This study specifically examines the synthesis of nonaggregated $CuInS_2$ (CIS) and its composite NCs, which have similar band-gap energy ($E_g = 1.5$ eV) to CdSe ($E_g = 1.7$ eV) and a high absorption coefficient. For those reasons, it has often been investigated for use in photovoltaic devices.[7] Some studies of chalcopyrite-type CIS NCs syntheses have been reported,[8] but no studies have found photoluminescence (PL) NCs at ambient temperature, except that of Castro et al.[8c] To obtain luminescence, defects and crystallinity control are critical: defects can trap excitons and thereby induce a nonemittable transition, causing low quantum yield. Therefore, NCs with high emission efficiency are inferred to offer high crystallinity with minimum defects. In addition, the scarcity of reports of PL NCs at ambient temperature for this material system indicates the difficulties posed by defects and crystallinity control of this multinary semiconductor. Castro et al. used a single molecular source and obtained a (PL) quantum yield of ca. 5%, but they were unable to tune the PL wavelength in a wide range[8c] despite their ability to control particle size within 2−4 nm (i.e., much smaller than the critical size for quantum effect (8.1 nm for CIS[8a])), although the reason for their difficulty remains unclear. Besides the quantum effect, alloying with other compounds, including chalcopyrite materials, is a common means to control bulk materials' electronic and magnetic properties.[9] For binary semiconductor NCs, in addition to the quantum size effects, alloyed semiconductor NCs[10] have recently been reported to tune their band-gap energy (E_g) and PL wavelength through band mixing. In addition, for semiconductor NCs, core−shell-type structures[11] in which the fluorescent NCs are covered with semiconductors with a higher E_g are often used to minimize the nonradiative transition to reduce the surface defect trapping to enhance PL intensity.

We specifically examined CIS NCs and their alloys and controlled their band-gap and optical properties through alloying them with Zn and Ga. From these NCs, we sought to obtain ambient temperature fluorescence with tunable E_g and PL.

Some straightforward methods for single molecular precursor preparation as a raw material source have been reported.[8d] However, for ease of expandability (i.e., ease in doping ratio control and in introducing variety of elements) and simplicity in preparation, we used inorganic Cu and In salts as starting materials for $CuInS_2$. We modified the high-temperature organic solvent method, which is often used for II−VI-type semiconductors.[1f]

Materials and Methods

As raw materials, copper(I) iodide, indium(III) iodide, and sulfur or diethyldithiocarbamide zinc (DECZn) were purchased from Sigma-Aldrich Corp.; octadecene (ODE) and oleylamine were also purchased from Sigma-Aldrich Corp. Aside from ODE, all reagents were used without further purification. For ODE, distillation was applied for purification.

NC preparations were conducted in a nitrogen atmosphere. We prepared three compounds: CIS, Zn-Cu-In-S, and ZnS−Zn-Cu-In-Ga-S.

For the Zn-Cu-In-S (ZCIS) system, 0.5 mmol of DECZn was dissolved in trioctylphosphine (TOP, 6 mL). The solution was diluted with ODE (24 mL) to render the DECZn concentration as 17 mmol/L. The solution was mixed with the oleylamine solution of copper and indium iodide, into which 0.2 mmol of CuI and the same molar amount of InI_3 were dissolved completely into 6 mL of oleylamine. Here, amine coordinates the Cu and In ions to produce amine complexes. These two material solutions were mixed to produce a raw material solution. After mixing these raw material

(4) (a) Miller, A.; Mackinnon, A.; Weaire, D. *Solid. State Phys.* **1981**, *36*, 119−175. (b) Contreras, M. A.; Egaa, B.; Ramanathan, K.; Hiltner, J.; Swartzlander, A.; F.; Hasoon, F.; Noufi, R. *Prog. Photovolt.* **1999**, *7*, 311. (c) Klenk, R. *Thin Solid Films* **2001**, *387*, 135. (d) Romero, M. J.; Ramanathan, K.; Contreras, M. A.; Al-Jassim, M. M.; Noufi, R.; Sheldon, P. *Appl. Phys. Lett.* **2003**, *83*, 4770. (e) Castro, S. L.; Bailey, S. G.; Raffaelle, R. P.; Banger, K. K.; Hepp, A. F. *Chem. Mater.* **2003**, *15*, 3142. (f) Tsuji, I.; Kato, H.; Kobayashi, H.; Kudo, A. *J. Phys. Chem. B* **2005**, *109*, 7323. (g) Tsuji, I.; Kato, H.; Kudo, A. *Angew. Chem.* **2005**, *44*, 3565.

(5) (a) Medvedkin, G. A. *Jpn. J. Appl. Phys.* **2000**, *39*, 949. (b) Zhao, Y.-J.; Geng, W. T.; Freeman, A. J.; Oguchi, T. *Phys. Rev. B* **2001**, *63*, 201202. (c) Zhao, Y. J.; Mahadevan, P.; Zunger, A. *Appl. Phys. Lett.* **2004**, *84*, 3753. (d) Erwin, S. C.; Zutic, I. *Nat. Mater.* **2004**, *3*, 410.

(6) (a) Osorio, R.; Bernard, J. E.; Froyen, S.; Zunger, A. *Phys. Rev. B* **1992**, *45*, 11173. (b) Wei, S. H.; Zunger, A. *J. Appl. Phys.* **1995**, *78*, 3846. (c) Song, H. K.; Jeong, J. K.; Kim, H. J.; Kim, S. K.; Yoon, K. H. *Thin Solid Films* **2003**, *435*, 186. (d) Albornoz, J. G.; Serna, R.; Leon, M. *J. Appl. Phys.* **2005**, *97*, 103515.

(7) (a) Bailey, S. G.; Flood, D. J. *Prog. Photovolt. Res. Appl.* **1998**, *6*, 1−14. (b) Schock, H. W.; Noufi, R. *Prog. Photovolt. Res. Appl.* **2000**, *8*, 151. (c) Contreras, M. A.; Egaas, B.; Ramanathan, K.; Hiltner, J.; Swartzlander, A.; Hasoon, F.; Noufi, R. *Prog. Photovolt. Res. Appl.* **1999**, *7*, 311. (d) Nanu, M.; Schoonman, J.; Goossens, A. *Adv. Mater.* **2004**, *16*, 453−456. (e) Siebentritt, S. *Thin Solid Films* **2002**, *403*, 1.

(8) (a) Czekelius, C.; Hilgendorff, M.; Spanhel, L.; Bedja, I.; Lerch, M.; Muller, G.; Bloeck, U.; Su, D. S.; Giersig, M. *Adv. Mater.* **1999**, *11*, 643. (b) Castro, S. L.; Bailey, S. G.; Raffaelle, R. P.; Banger, K. K.; Hepp, A. F. *Chem. Mater.* **2003**, *15*, 3142. (c) Castro, S. L.; Bailey, S. G.; Raffaelle, R. P.; Banger, K. K.; Hepp, A. F. *J. Phys. Chem. B* **2004**, *108*, 12429. (d) Banger, K. K.; Jin, M. H.-C.; Harris, J. D.; Fanwick, P. E.; Hepp, A. F. *Inorg. Chem.* **2003**, *42*, 7713−7715.

(9) (a) Klenk, R.; Klaer, J.; Scheer, R.; Lux-Steiner, M. C.; Luck, I.; Meyer, N.; Ruhle, U. *Thin Solid Films* **2005**, *480*, 509. (b) Tanaka, T.; Demizu, Y.; Yamaguchi, T.; Yoshida, A. *Jpn. J. Appl. Phys., Pt. 1* **1996**, *35*, 2779. (c) Nomura, R.; Skel, Y.; Matsuda, H. *J. Mater. Chem.* **1992**, *2*, 765. (d) Negami, T.; Kohara, N.; Nishitani, M.; Wada, T.; Hirao, T. *Appl. Phys. Lett.* **1995**, *67*, 85. (e) Oja, I.; Nanu, M.; Katerski, A.; Krunks, M.; Mere, A.; Raujoja, J.; Goossens, A. *Thin Solid Films* **2005**, *480*, 82. (f) Chun, Y. G.; Kim, K. H.; Yoon, K. H. *Thin Solid Films* **2005**, *480*, 46.

(10) (a) Takeoka, S.; Toshikiyo, K.; Fujii, M.; Hayashi, S.; Yamamoto, K. *Phys. Rev. B* **2000**, *61*, 15988. (b) Malik, M. A.; O'Brien, P.; Revaprasadu, N. *Chem. Mater.* **2002**, *14*, 2004. (c) Zhong, X. H.; Feng, Y. Y.; Knoll, W.; Han, M. Y. *J. Am. Chem. Soc.* **2003**, *125*, 13559. (d) Weissker, H. Ch.; Furthmuller, J.; Bechstedt, F. *Phys. Rev. Lett.* **2003**, *90*, 085501. (e) Schulli, T. U.; Stangl, J.; Zhong, Z.; Lechner, R. T.; Sztucki, M.; Metzger, T. H.; Bauer, G. *Phys. Rev. Lett.* **2003**, *90*, 066105. (f) Shavel, A.; Gaponik, N.; Eychmuller, A. *J. Phys. Chem. B* **2004**, *108*, 5905. (g) Zhong, X. H.; Zhang, Z. H.; Liu, S. H.; Han, M. Y.; Knoll, W. *J. Phys. Chem. B* **2004**, *108*, 15552.

(11) (a) Dabbousi, B. O.; Rodrigez-Viejo, J.; Mikulec, F. V.; Heine, J. R.; Mattoussi, H.; Ober, R.; Jensen, K. F.; Bawendi, M. G. *J. Phys. Chem. B* **1997**, *101*, 9463. (b) Talapin, D. V.; Rogach, A. L.; Komowski, A.; Hasse, M.; Weller, H. *Nano Lett.* **2001**, *1*, 207. (c) Lifshitz, E.; Fradkin, L.; Glozman, A.; Langof, L. *Annu. Rev. Phys. Chem.* **2004**, *55*, 509. (d) Kim, S.; Fisher, B.; Eisler, H. J.; Bawendi, M. *J. Am. Chem. Soc.* **2003**, *125*, 11466. (e) Son, D. H.; Hughes, S. M.; Yin, Y. D.; Alivisatos, A. P. *Science* **2004**, *306*, 1009.

solutions, the composition ratios of Cu and In were variable from 0.5 to 5. Those of Zn and S were fixed, indicated as Zn:Cu:In:S = 1:*n*:*n*:4 ($n = 0.5-5$). For $n = 1$, the compounds' concentrations were 11 mmol/L for Cu and In ions and DECZn (contains four sulfur atoms for one molecule). The 2 mL of raw material solution was put into a 10 mL test tube and soaked directly in an oil bath that had been preheated to 160−280 °C and aged for 60−300 s. The DECZn decomposed to ZnS at a sufficient rate when heated to 150 °C or higher temperatures.[12] Excess sulfur reacts with copper and indium iodide to generate ZCIS. The prepared solutions were clear red or brown, reflecting their high colloidal stability.

Preparation of simple CIS and Zn−Cu−In−Ga−S was achieved through modifying the above reaction system. Sulfur (0.4 mmol) was dissolved into TOP to substitute DECZn and prepare a simple CIS. For the case of Zn−Cu−In−Ga−S system, GaI_3 was introduced to the amine solution while maintaining the total concentration of InI_3 and GaI_3 constant (0.2 mmol). In neither case did the product solutions show turbidity.

For optical analyses, these prepared solutions were diluted with chloroform to an optical density around 0.1−0.2. Then UV−vis, PL emission, and excitation (PLE) spectroscopy were applied using a UV−vis spectrophotometer (UV-1600; Shimadzu Corp., Japan) and a spectrofluorometer (FP-6600; Jasco, Inc., Japan). The PL quantum yields were determined by comparing the integrated emission of the samples to that of rhodamine B in solution with an excitation wavelength of 400 nm.

Morphological and structural analyses were undertaken using X-ray diffraction analysis (XRD, PW1710; Philips Co.), scanning transmission electron microscopy (STEM, S-5200, Hitachi high technologies Co., Japan), and high-resolution transmission electron microscopy (HR-TEM, Tecnai-20F; FEI Corp.). For detailed XRD analyses, high-energy XRD was also applied at Spring8. For these observations the products were precipitated with alcohol. They were further isolated by centrifugation to remove excess surfactants. The centrifuged particles were redispersed into an organic solvent like toluene to yield a clear, colloidally stable suspension. The washed sample was also used to analyze Cu and Zn contents in the NCs, which were determined using inductive coupling plasma atomic emission spectrometry (ICP-AES).

Results and Discussion

We prepared simple $CuInS_2$ nanocrystals (NCs). Images of TEM and XRD spectra (Supporting Information 1, Figures 1 and 2) revealed that the product was discrete $CuInS_2$ NCs with 3.5 nm average particle for a 160 °C reaction temperature. Its diameter increased to 7.5 nm at 240 °C. The sample's absorption spectrum (Supporting Information, Figure 3) showed a typical curve for a semiconductor with an absorption edge, but the band-edge absorption peak is rather vague and located around 650 nm (1.9 eV). From CIS NCs, only a slight PL around 730 nm was observed at room temperature. The quantum yield was low (<0.1%), which probably reflects the difficulty in defect control, as described in the Introduction.

In a chalcopyrite $CuInS_2$ (CIS), the Cu−S bond is weaker than that of In−S and the Cu vacancy is preferably generated. In addition, the Cu vacancies induce anti-site defect generation.[13] The ionic diameter of Zn is similar to that of Cu and preferentially substituted to Cu; the Zn substitution of Cu was shown to be energetically favorable to prevent anti-site defects.[13] Therefore, introduction of Zn ion into these CIS NCs was expected to improve the PL intensity. Furthermore, Luck et al. reported that the band-gap energy (E_g) of mixed crystals of ZnS−$CuInS_2$ (ZCIS) offers advantages for variation at room temperature of 3.67 (ZnS) to 1.55 eV ($CuInS_2$).[14] Therefore, to obtain PL wavelength-tunable NCs with a rather high quantum yield, which has not been achieved for the chalcopyrite-type NCs to date, we attempted alloying $CuInS_2$ with ZnS to produce ZCIS NCs.

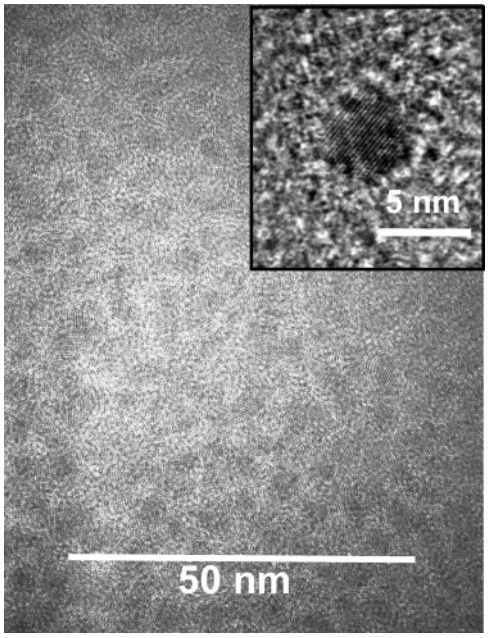

Figure 1. TEM image of ZCIS nanocrystals (Zn:Cu:In:S = 1:1:1:4).

Figure 1 shows a TEM image of ZCIS NCs from Zn:Cu:In:S = 1:1:1:4. As shown, about 3.5 nm well-crystallized discrete particles were observed using TEM. In addition, XRD analyses (Figure 3) showed diffraction peaks located between those for cubic ZnS peak and the tetragonal CIS peak,[15] showing no discrepancy with ZnS−CIS alloying using the current synthesis method.

Figure 2 shows the UV−vis, PL, and PLE characteristics of the product. The UV−vis spectrum shows a typical curve of a semiconductor material: a band-edge peak was visible at around 530 nm (ca. 2.3 eV). It is considerably larger than that of the simple CIS NCs prepared in this study (1.9 eV). The PL emission was observed around 630 nm with a full-width at half-maximum (fwhm) of about 130 nm; the Stokes shift was almost 120 nm. One reason for the wide fwhm is the wide particle size distribution. Size-selective precipitation of the product[1c] or synthesis by a microfluidic reactor, as described in ref 1g, was able to reduce the particle size distribution and thereby reduce the fwhm to 80−100 nm. However, it was larger than that for the PL peak of II−VI semiconductors from the band edge.[1] The PLE spectrum for 630 nm emission showed good correspondence with the

(12) Wang, H.; Nakamura, H.; Yamaguchi, Y.; Uehara, M.; Miyazaki, M.; Maeda, H. *Adv. Funct. Mater.* **2005**, *15*, 603.

(13) Yamamoto, T.; Luck, I. V.; Scheer, R.; Katayama-Yoshida, H. *Physica B* **1999**, *274*, 927.

(14) Luck, I.; Henrion, W.; Scheer, R.; Doering, T.; Bente K.; Lewerenz, H. *J. Cryst. Res. Technol.* **1996**, *31*, 841.

(15) Luck, I.; Fieber-Erdmann, M.; Teichert, B.; Scheer, R.; Holub-Krappe, E.; Lewerenz, H.-J. *Inst. Phys. Conf. Ser.* **1997**, *152B*, 385.

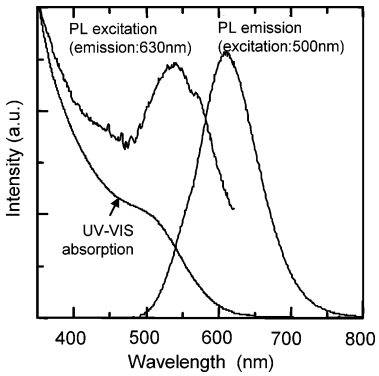

Figure 2. UV−vis absorption, PL emission (excitation at 500 nm), and excitation (emission at 630 nm) spectra of CIS−ZnS nanocrystal solution (Zn:Cu:In:S = 1:1:1:4).

Table 1. Cu/Zn Molar Ratio in the Reaction Solution and Product, Average Particle Size, and Molar Extinction Coefficient at the Band-Edge Absorption Peak of the Product

reaction temperature			200			160	300
Cu/Zn ratio in reaction solution	0.5	1	2	3	5	1	1
Cu/Zn ratio in the product	0.12	0.38	0.9	1.6	2.7	0.35	0.7
particle size (nm)	2.6	3.5	4.5	4.4	4	1.9	3.9
lattice constant (Å)		5.48	5.51		5.53		

absorption peak, indicating that the PL is related to the semiconductor band gap. The quantum yield for Zn−Cu−In−S (ZCIS) was ca. 5%, which is much greater than that shown by CIS NCs prepared using a similar method. This marked improvement in QY indicates that alloying of ZnS with CIS NCs would be effective to enhance the PL intensity, as expected. The wide fwhm peak and large Stokes shift resembled those reported by Castro et al.,[8c] indicating that PL is derived mainly from the donor−acceptor (D−A) transition. Additional ZnS coating on the ZCIS NCs to eliminate surface defects almost doubled the PL intensity without a PL wavelength shift (see Supporting Information for procedural and experimental data) as was often reported for other semiconductor NCs.[11] However, the wide PL peak and large Stokes shifts were not reduced, indicating that the D−A transition results not from surface defects but from intrinsic defects.

In the next step, we attempted to control the PL wavelength and band-gap energy by controlling the CIS/ZnS ratio. The CIS/ZnS ratio was controlled by controlling the raw material composition. In this study, the molar ratio of Cu (═In) to Zn in the raw material solution was varied from 0.5 to 5, as indicated in this report as Zn:Cu:In:S = 1:*n*:*n*:4 (*n* = 0.5−5). The mixed raw materials solution was heated at 200 °C for 300 s. The average particle sizes obtained were 2.4−4.5 nm; the size was tunable through changing the reaction condition, as shown in Table 1, which also shows that the Cu/Zn ratio of the product determined by ICP corresponds well with that of the raw material solutions. Reaction temperatures also affect the Cu/Zn ratio and particle size. The mismatch between the Cu/Zn ratio in the reaction solution and the product mostly arises from the coordination equilibrium of the metal complex and the difference in the reaction rate. Table 1 also indicates lattice constants of products *n* = 1, 3, and 5, as determined by high-energy X-ray diffraction at Spring8. (Figure 3). The lattice constants of

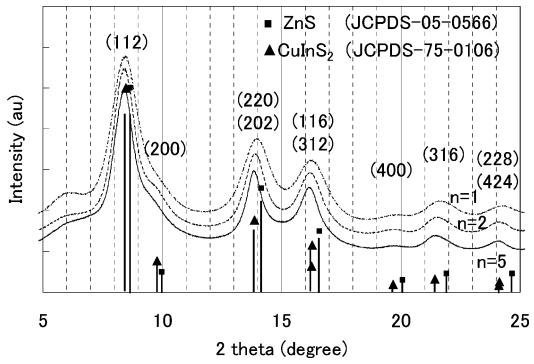

Figure 3. XRD spectra of nanocrystals from various raw material compositions (Zn:Cu:In:S = 1:*n*:*n*:4). Black lines and gray lines on the *X*-axis, respectively, denote CuInS2 and ZnS diffraction patterns.

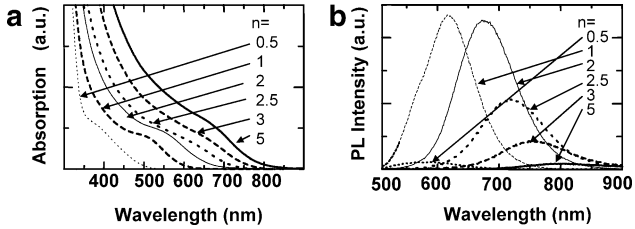

Figure 4. Raw material composition effects on optical properties: (a) UV−vis absorption and (b) PL emission spectra (excitation 500 nm). (Raw material composition Zn:Cu:In:S = 1:*n*:*n*:4 (*n* = 0.5−5).)

the *a* axis increased with Cu content. They almost agree with those of the ZnS molar ratio for bulk system,[16] assuming that the composition was controlled using the current method.

Figure 4a portrays UV−vis spectra of these products. By increasing the Cu(═In) ratio in the reaction solution (i.e., decreasing the Zn ratio), the absorption edge shifted from ca. 400 (3.1 eV) to ca. 700 nm (1.8 eV) toward the longer wavelength, as expected. The band-gap energy is considerably larger than the reported value for bulk ZCIS; (2.1−1.5 eV for the same Cu/Zn range).[17]

Figure 4b shows that the PL peak was also controllable within 550−800 nm with the starting composition. The highest PL intensity was afforded by *n* = 1−2; their quantum yields were around 5%. When Cu/Zn of the reaction solution was 1−5, the particle size was 4 ± 0.5 nm, but the PL wavelength varied from 620 to 800 nm (optical band gap varied 2.5−1.8 eV), thereby demonstrating tuning of the PL wavelength by the current method using a constant particle size.

Figure 5a shows optical band-gap energy (E_g) dependency on the Cu/Zn ratio shown in Table 1. The optical band gap of bulk ZCIS[14] (translated into Cu/Zn ratio) is also shown in Figure 5a. In that figure the E_g for ZCIS NCs also increases with the decreasing Cu/Zn ratio, but the value is considerably higher than that of bulk ZCIS. The product particles were much smaller than the critical size for quantum effect of $CuInS_2$ (8.1 nm)[8a] and that of ZnS (5.0 nm).[18] Therefore, the quantum size effect, along with the contribut-

(16) Parasyuk, O.; Voronyuk, S.; Gulay, L.; Davidyuk, G.; Halka, V. *J. Alloys Compd.* **2003**, *348*, 57.
(17) Bente, K.; Wagner, G.; Lazar, M.; Lange, U.; Doering, T.; Rao, K. V.; Zehnder, T.; Luck, I.; Lewerenz, K.-J. *Inst. Phys. Conf. Ser.* **1997**, *152*, 935.
(18) Rossetti, R.; Hull, R.; Gibson, J.; Brus, L. *J. Chem. Phys.* **1985**, *82*, 552−559.

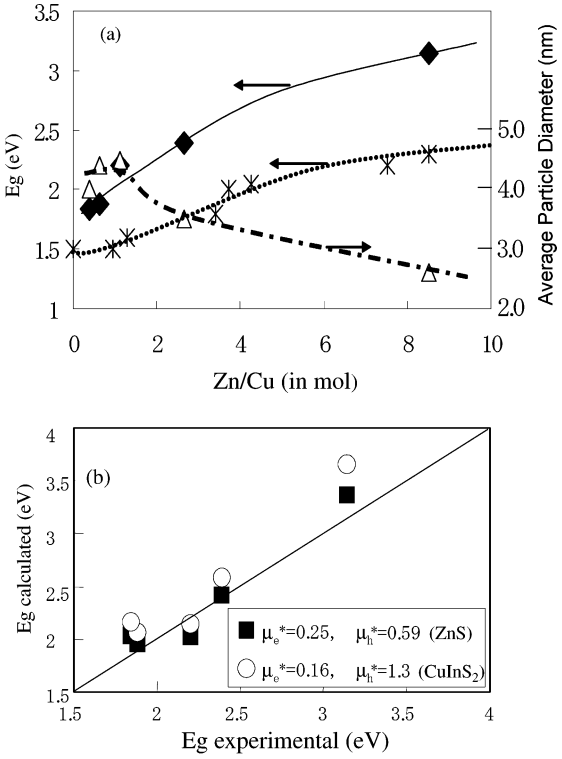

Figure 5. (a) Band-gap energy (E_g) (◆) and particle size diameter (△) dependency on ZCIS composition (Zn/Cu molar ratio). Bulk E_g data from ref 40 are also shown with an asterisk (*). (b) E_g comparison of experimental and calculated values of the effective mass approximation. For calculations, the effective mass was used for $CuInS_2$ (○) and ZnS (■).

ing effect of ZnS, is considered to be responsible for the wider band-gap energy of this product than that of bulk $CuInS_2$ materials. From this point of view, we estimated the band gap using an effective mass approximation method[19]

$$E_{gcal} = E_{g\,bulk} + (k_B{}^2\pi^2/2R^2)(1/\mu_e{}^* + 1/\mu_h{}^*) - 1.8\ e^2/\epsilon R \quad (1)$$

where $E_{g\,bulk}$ is the band-gap energy of bulk material, k_B represents the Boltzman constant, R is the NC radius, $\mu_e{}^*$ denotes the effective mass of the electron, $\mu_h{}^*$ is the effective hole mass, and ϵ is the dielectric constant. The contribution of the second term was not large for this case, but the contribution of effective mass was not negligible. We found only slight composition dependence data of $\mu_e{}^*$ and $\mu_h{}^*$ for ZCIS. Therefore, we estimated E_g using those values for ZnS ($\mu_e{}^* = 0.25$, $\mu_h{}^* = 0.59$)[18] and CIS ($\mu_e{}^* = 0.16$, $\mu_h{}^* = 1.3$),[8a] as shown in Figure 5b. The effective mass is inferred to shift from those for CIS to ZnS by increasing the Zn/Cu ratio (i.e., higher E_g in the figure). The lattice constant shown in Table 1 is possible for some composite structures such as a completely mixed solution, a core−shell structure, or graduated structure, as shown in the inset of Figure 5b, but the calculated value shows good correspondence with the experimental value, which would show that the product particles are rather mixed crystal type and the optical band gap is affected by both band mixing of ZnS and CIS and quantum effect.

As described above, the band gap and PL peak location were controlled by introducing Zn(II) into the Cu−In−S system. For further control of the PL wavelength to cover the whole of the visible light wavelengths, we introduced Ga(III) ions to the current system. In this case, Zn and Cu concentrations in the raw material solution were made constant, and Ga+In was made to be the same content with Cu (=Zn). The In:Ga ratio was varied from 1:0 to 0:1. Mixed solutions of these elements were produced similarly to ZCIS and heated at 280 °C for 5 min. The XRD result of the product (see Supporting Information Figure 6) shows a peak shift toward narrower lattice spacing with increasing Ga content, indicating alloying. The UV−vis absorption spectrum shown in Figure 6 indicates an absorption edge shift toward shorter wavelength (i.e., wider band-gap energy) with substitution of In(III) for the lighter element Ga(III) until complete substitution (λ_{abs} of ca. 400 nm (3.0 eV)). The PL peak wavelength also shifts to a shorter wavelength: from 700 to 480 nm. These results demonstrate wide tunability in chalcopyrite-type nanoparticles using elemental selection.

Finally, we attempted surface modification of ZCIS NCs using mercaptoundecanoic acid based on the reported method for CdSe[20] (see Supporting Information V for hydrophilization method). We redispersed the ZCIS NCs into mercaptoundecanoic acid (MUA) (with a slight amount of toluene) and exchanged the surface. The MUA has two functions: thiol and carboxyl. Because the metal ions (i.e., Zn(II) and Cu(I)) on the surface of ZCIS NCs have higher binding constants with thiol than with carboxyl functions, the carboxyl part tends to exist on the outer surface. Adjusting the pH of the solution above pK_a of the carboxyl part by alkaline addition, the surface will have a charge to disperse the NCs in the water. We obtained an aqueous colloid of ZCIS. Optical properties of hydrophilic ZCIS NCs showed no marked difference from those before surface modification. This result and high absorption coefficient of the material illustrate this material's high potential for use as a fluorescent tag for biological molecules.

Summary

Using a simple solution method, we demonstrated control of optical properties, band-gap energy, and PL wavelength through alloying processes of chalcopyrite-type nanocrystals (NCs): Zn−Cu−In−S (ZCIS) and Zn−Cu−In−Ga−S (ZCIGS). Introducing Zn to $CuInS_2$, it became possible to improve the PL intensity to an extreme degree to achieve an optical quantum yield = 5%. Light emission was tunable within 550−800 nm and controlled by composition, indicating alloying in the ZCIS system. Moreover, additional ZnS coating doubled the PL intensity without a peak shift. The product was hydrophilized easily, similarly to CdSe NCs. In addition, the elemental ratio in the reaction solution yields various NCs with identical particle size. Moreover, substitution of In(III) with Ga(III) enabled tuning of E_g and PL wavelengths toward shorter wavelengths as short as 480 nm.

The wide selectivity in components and composition by this method suggest a new series of chalcopyrite-type

(19) Brus, L. E. *J. Phys. Chem.* **1986**, *90*, 2555.

(20) Hanaki, H.; Momo, A.; Oku, T.; Komoto, A.; Maenosono, S.; Yamaguchi, Y.; Yamamoto, K. *Biochem. Biophys. Res. Commun.* **2003**, *302*, 496.

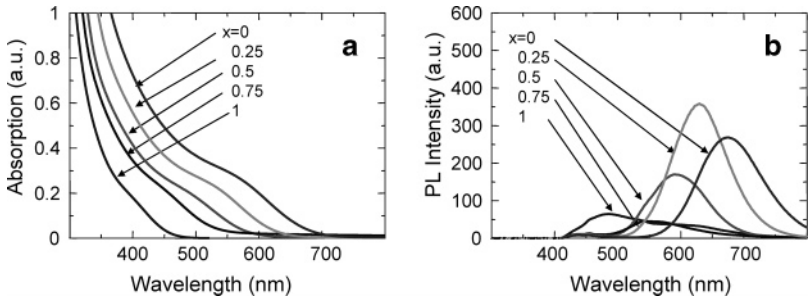

Figure 6. Composition effects on optical properties of Zn−Cu−In−Ga−S NCs: (A) UV−vis absorption and (B) PL emission spectra (excitation 500 nm). (Zn:Cu:In:Ga:S = 1:1:(1 − *x*):*x*:4 (*x* = 0, 0.25, 0.5, 0.75, 1)).

semiconductor NCs with various properties. These materials would be useful alone or as building blocks for fluorescent materials, light absorbers for solar cells, or other electric devices, photocatalysts, and spintronics materials, as reported for singular or binary semiconductors, but with much wider variation. In addition, the material's nonregulated status, it uses no Cd, Pb, or Hg, and simple synthesis offer advantages for use in visible and near-IR lighting.

Acknowledgment. Part of this study was supported by the Industrial Technology Research Grant Program (02A38001c) from the New Energy and Industrial Technology Development Organization (NEDO) of Japan. In addition, the "Nanotechnology Support Project" of the Ministry of Education, Culture, Sports, Science and Technology (MEXT) supported the TEM analyses presented herein. High-energy XRD was performed at Spring8.

Supporting Information Available: Additional figures and text. This material is available free of charge via the Internet at http://pubs.acs.org.

CM0518022